



MVMoO₇ SUBSTITUTED PHASES (M=Fe, Cr): STRUCTURAL STABILITY, REDUCIBILITY AND CATALYTIC PROPERTIES IN METHANOL OXIDATION

Irma L. Botto^{1*}, Marta Vassallo¹, Mercedes Muñoz², Carmen I. Cabello^{2#} and Luis Gambaro².

¹CEQUINOR, CONICET-La Plata, Facultad de Ciencias Exactas, Universidad Nacional de La Plata, 47 esq. 115, (1900) La Plata, Argentina.

²CINDECA, CONICET -La Plata, Facultad de Ciencias Exactas, Universidad Nacional de La Plata, 47 N° 257, (1900) La Plata, Argentina. # Member CICPBA.

*E mail: botto@quimica.unlp.edu.ar FAX: 54-221-4259485

Received December 22, 2008. In final form February 22, 2009.

Abstract

Structural, spectroscopic and thermal properties of MVMoO₇ (M= Fe, Cr) phases, of potential interest in the catalysis field, are studied by means of X-ray Powder Diffraction XRD, Fourier Transformed Infrared Spectroscopy FTIR, Electronic Scanning Microscopy and X Ray Energy Dispersive Scattering Micro-Analysis SEM-EDS and Temperature Programmed Reduction TPR techniques. Thus, the formation of a triclinic solid solution in a complete range of composition is supported by a little M(III) size difference (about 5 %). In relation to the thermal reduction behaviour, iron is the unique reducible trivalent species. The reduction products of the Fe-Cr solid solution seem to be governed by the structural arrangement and particularly by the presence of M₂O₁₀ dimmers. The results are analyzed and compared with TPR data of MoO₃, V₂O₅, M₂O₃,

$M_2(MoO_4)_3$ and MVO_4 (M= Fe, Cr) binary and ternary systems. For the Fe-end member of the isomorphous series, a part of iron remains unreduced as FeV_2O_4 –spinel phase at 1000°C whereas $(V,Cr)_2O_3$ is the final oxidizing product for the Cr-end member. However, the $(Fe_{0.5}Cr_{0.5})VMoO_7$ reduction occurs through the formation of $FeMoO_4$ intermediate, affecting the Mo(VI)-Mo(IV)-Mo stability field and the V(V)-V(III) reduction steps. Finally, $MVMoO_7$ (M= Fe, Cr) phases are chemically proved in the methanol oxidation reaction by Transients Study and the relationships among structural and chemical features and the catalytic behaviour are analyzed and discussed.

Keywords: $MVMoO_7$ (M= Fe, Cr), triclinic solid solution, thermal programmed reduction, transients study, methanol oxidation.

Resumen

Se reportan las propiedades estructurales, espectroscópicas y térmicas de fases de fórmula: $MVMoO_7$ (M= Fe, Cr), de potencial interés en el campo de la catálisis. El estudio se realizó mediante técnicas como Difracción de Polvos por Rayos X, (DRX), Espectroscopía de Infrarrojo por Transformada de Fourier, (IRTF), Microscopía electrónica de Barrido y Microanálisis por Energía Dispersiva de Rayos X, (MEB) y técnicas de reducción térmica programada (RTP). La formación de una solución sólida triclínica en un rango completo de composición depende de una pequeña diferencia (5%) en el tamaño de M(III). Respecto al comportamiento en la reducción térmica, el Fe(III) fue la única especie trivalente reducible. Los productos de reducción de la solución sólida Fe-Cr parecen depender del ordenamiento estructural y especialmente de la presencia de dímeros M_2O_{10} . Los resultados fueron analizados y comparados con datos de RTP de sistemas binarios y ternarios como MoO_3 , V_2O_5 , M_2O_3 , $M_2(MoO_4)_3$ y MVO_4 (M= Fe, Cr). Para el miembro final de Fe de la serie isomorfa, una parte del Fe permanece sin reducir como la fase espinela FeV_2O_4 a 1000 °C, mientras que $(V,Cr)_2O_3$, es el último producto oxídico para el miembro final de Cr. Sin embargo, la reducción de $(Fe_{0.5}Cr_{0.5})VMoO_7$ ocurre a través de la formación del intermediario $FeMoO_4$, afectando el campo de estabilidad de Mo(VI)-Mo(IV)-Mo y las etapas de reducción del V(V)-V(III). Finalmente las fases $MVMoO_7$ (M= Fe, Cr) fueron evaluadas en la reacción de oxidación de metanol mediante el Estudio de Transientes. Se analizó y discutió el comportamiento catalítico en relación a las propiedades químicas y estructurales.

Palabras clave: $MVMoO_7$ (M= Fe, Cr), solución sólida triclínica, reducción térmica programada, estudio de transientes, oxidación de metanol.

Introduction

Bimetallic oxides as well as mechanical mixtures involving components of the MoO_3 - Fe_2O_3 system have long been the focus of industrial interest as oxidation catalytic materials [1-4]. The basis of a great number of petrochemical processes is an oxidation reaction, performed in a range of temperature between 300-600 °C. This involves the substrate oxidation which is followed by the regeneration of the oxometal-catalyst by reaction of its reduced form with molecular oxygen [4].

Regarding the catalytic activity and selectivity, the easily reducible catalysts (strong oxidants) are active but non-selective in producing an extensive degradation to CO_2 . At the other extreme, metal oxides that are difficult to reduce are deemed inactive. So, only those metal oxides of intermediate reducibility (i.e. moderate oxidants) are considered to be capable of producing selective oxidation. In this sense, the activity-selectivity observed in certain combination of simple and mixed oxides are successful in catalytic oxidations of olefins [4].

Much attention is focused on the promoting effect of transition metals with mild redox conditions such as iron, copper, chromium, cobalt or nickel. The synergism shown by the

multiphasic-monometallic and monophasic-multimetallic catalytic systems is basically related to the fast electron transport and oxygen mobility [5].

Some phases of the M₂O₃-MoO₃-V₂O₅ (M= Al, Fe, Cr) system with MVMoO₇ composition have been prepared by heating mixtures of binary oxides or precursors up to 700 °C [6- 8] but only CrVMoO₇ and FeVMoO₇ are isomorphous [8]. Cr(III)-Fe(III) substitution in oxide systems is favoured by the similarity of both ionic radii (0.645 Å for Fe(III) and 0.615 Å for Cr(III)) [9]. So, the formation of solid solutions is expected to be possible in a whole range of composition. The replacement of both Cr(III) and Fe(III) ions by Al(III) is more difficult to be observed due to the lower radius of the latter (0.535 Å) [9, 10] and thus, the AlVMoO₇ phase can be classified as a polyoxovanadate, crystallizing in a different way.

The MVMoO₇ isomorphous system seems to be interesting from the catalytic point of view because the potential synergism among the metals. Badlani et al. [11] studied the interaction of V₂O₅, MoO₃, Fe₂O₃ and Cr₂O₃ binary oxides with methanol and concluded that the two firsts oxides were characterized by the redox properties, the iron oxide by redox and acid properties and the latter by more acidic than redox properties.

The aim of this work is the study of the potentiality of the (Cr,Fe)VMoO₇ solid solution as oxidation catalysts from the analysis of structural and thermal reduction stability. This is supported by Temperature Programmed Reduction technique (TPR) with the aid of the X-ray diffraction analysis, FTIR spectroscopy, and the electron microprobe analysis (SEM-EDS). The comparison with the reduction behaviour of related molybdates and vanadates was made to elucidate the intermediate products of thermal reduction. The MVMoO₇ catalytic behaviour was evaluated by the Study of Transients in the methanol oxidation. Finally, structural, compositional and catalytic properties are correlated.

Experimental

CrVMoO₇ and FeVMoO₇ phases were obtained as described somewhere else [12]. Triclinic Fe_{1-x}Cr_xVMoO₇ solid solution was obtained by using V₂O₅ (Merck p.a.), α-Fe₂O₃ (Merck p.a.), (NH₄)₂Cr₂O₇ (Mallinckrodt p.a.) and (NH₄)₆Mo₇O₂₄·7H₂O (M&B p.a.) as starting materials in the stoichiometric ratio. Successive thermal steps at 600°C (24h), 650°C (72 h) and 700°C (24 h) led to pure phases.

Bimetallic and monometallic oxides (M₂(MoO₄)₃, MVO₄, V₂O₅, MoO₃ and M₂O₃ where M= Fe, Cr) were prepared and used for comparative purposes.

All crystal phases were identified by XRD analysis, using a Philips PW 1714 diffractometer (Cu Kα radiation, Ni filtered). Cell parameters were refined by the UNITCEL program [13]. NaCl was employed as external standard.

FTIR spectra were registered in a Bruker IFSS 66 (FTIR) spectrophotometer (KBr pellet technique).

Samples were also analyzed by SEM- EDS scanning electron microscopy (Philips 505, EDAX 9100 equipment). Additional surface area measurements by BET technique was done in a Micromeritics ASAP 2020 equipment,

Reduction studies were carried out by means of TPR technique. The home-made reactor was fed with a 10 % H₂ reducing agent in a N₂ stream (55 cm.min⁻¹) from 20 to 1050 °C. Heating rate was 5 °C min⁻¹. The hydrogen consumed was detected by a thermal conductivity cell. Additional thermal studies were carried out in reducing conditions (similar to those of TPR experiments) and in air atmosphere by means of a controlled temperature furnace.

Transients measurements from the surfaces of multimetallic phases were carried out in an ultra-high vacuum surface analysis reactor (base pressure ~ 1.33 10⁻⁵ Pa).

Two detectors were used: catarametric cell (Shimadzu GC-8A), employed as real time detector and Balzers QMG 112A Mass Quadrupole, to control the composition of reaction products. By means of high speed data acquisitions and ad hoc programs, the different mass intensities could be plotted in function of reactive pulses.

The transients were studied, by means of ≈ 100 mg of solids by injecting 5 methanol pulses of $0.5 \mu\text{l}$ at 400°C in a He flow of 99.999 % of purity, detecting reaction products and unreacted methanol by Mass Spectrometry.

Results and discussion

I- Structural stability

The isomorphous FeVMoO_7 - CrVMoO_7 system is a 3D structural framework which results from the connection of different polyhedron in a triclinic unit cell. The trivalent metals are located in an octahedral oxygen environment while Mo and V are tetrahedrally coordinated. Pairs of MO_6 are connected by a common edge forming $(\text{M}_2\text{O}_{10})$ dimers whereas VO_4 groups are corner-linked to these units. However, tetrahedral symmetry is lowered by the presence of a very short V-O bond length ($\sim 1.59 \text{ \AA}$), another intermediate one of 1.68 \AA and two longer ones of 1.76 and 1.85 \AA as it is observed in the CrVMoO_7 structure [8]. The layer-like nets are linked together in the perpendicular direction by three corners of MoO_4 tetrahedra. These last moieties also show a $\text{Mo}=\text{O}$ shorter bond ($\sim 1.64 \text{ \AA}$), lower than the other three ones ranged between 1.74 - 1.78 \AA) [8]. Slight distortions of the coordination polyhedron result from the connectivity, high condensation and different polarizing effect of metal atoms. Fig. 1 shows an “ideal” projection of the described structure (simplified from reference 8), which is constituted by M(III)-V layers (named A) and relatively free chains of MoO_4 groups (named B) which are the cohesion between the layers.

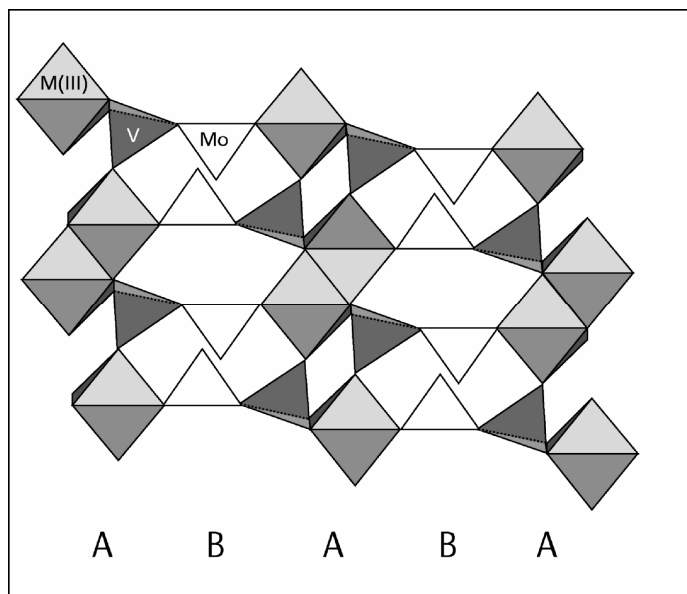


Figure 1. “Ideal” projection of MVMoO_7 structure.

The XRD analysis of the $\text{Fe}_{1-x}\text{Cr}_x\text{VMoO}_7$ solid solution revealed the existence of a single phase for every x value. Cell parameters calculated for the referring $x=0.5$ phase led to a cell volume of $278.9(5) \text{ \AA}^3$, intermediate between that calculated for Fe- and Cr- end members and with those reported in literature for FeVMoO_7 and CrVMoO_7 [8]. The diminution of the triclinic unit cell

volume with increasing chromium content was in agreement with the decrease of M(III) ionic radii. So, although the high condensation of the structure, a difference of ~ 5 % in M(III) size is enough to form the solid solution over the whole range of concentration.

The assignment of FTIR bands showed in Table 1 was performed from the structural feature. Typical FTIR spectrum of the Cr rich end member of the series is shown in Fig. 2. A clear trend to lower frequencies is observed with the increase of the Fe content. The shorter V-O bonds were shifted from 980 and 948 to 975 and 943 cm⁻¹ respectively, whereas the shortest Mo-O stretching mode vary between 902 and 887 cm⁻¹. The broad and strong bands between 848 and 727 for x = 1 and 798 and 692 cm⁻¹ for x = 0 can be assigned to the remaining Mo and V tetrahedral bonds. The reinforcement of the Mo-O and V-O stretching bonds, is associated to the unit cell contraction by the effect of the trivalent replacement.

Table 1. FTIR spectra of the Cr_xFe_{1-x}VMoO₇ (in cm⁻¹).

x = 0	x = 0.5	x = 1	Assignment
975 sh 943 s	976 m 945 s	980 s 948 s	vV-O (shorter bonds)
887 s	893 s	902 s	vMo-O (shortest)
798 vs	830 vs	848 vs	v Mo-O and
		800 sh	vV-O
692 vs (br)	709 s	727 s	(see text)
	600 sh		
494 m	524 m	536 m	v M(III)-O
458 w	469 sh	470 w	
400 sh	415 sh	421 sh	δ Mo-O,
395 w	396 m	404 s	δ V-O
371 w	368 vw	361 w	δ M(III)-O
340 w	350 sh	351 w	
		338 w	Lattice modes
310 w	300 sh	306 m	

s (strong), vs (very strong), m (medium), w (weak), br (broad), sh (shoulder)

The bands in the 500 cm⁻¹ region (536, 524 and 494 cm⁻¹ for x = 1, 0.5 and 0 respectively) assigned to the M(III)-O stretching modes, were located at lower wavenumbers than those observed in Fe₂O₃, Cr₂O₃ and related oxides [10, 14,15], which can be associated to the condensation effects

in the lattice. Nevertheless, a subsequent shifting of the bands to higher values with increasing x was also in agreement with the general trend, observed in the well studied $(\text{Fe}_{1-x}\text{Cr}_x)_2\text{O}_3$ solid solution [15,16]. The assignment was more difficult below 500 cm^{-1} where the vanadium, molybdenum and Fe/Cr-bending modes as well as the lattice vibrations were expected.

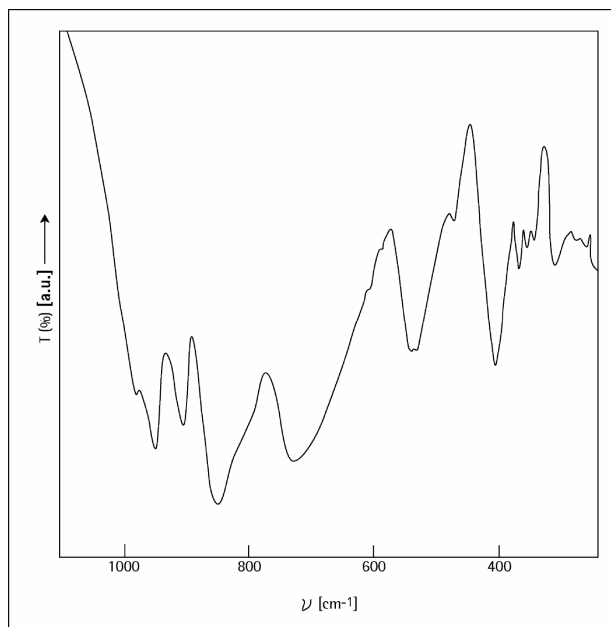


Figure 2: FTIR spectrum of CrVMoO_7 (range 1200 to 200 cm^{-1}).

II- Thermal stability

The comparison of TPR profiles for three members of the $(\text{Cr,Fe})\text{VMoO}_7$ solid solution is shown in Fig. 3 (a-c). Patterns corresponding to $\text{Cr}_2(\text{MoO}_4)_3$, $\text{Fe}_2(\text{MoO}_4)_3$, FeVO_4 and CrVO_4 phases (in similar experimental conditions) were also included in the figure with comparative purposes. On the basis that the global reduction process in a multimetallic system is affected by the reducibility of each component, it is also essential to take into account the reduction behaviour of MoO_3 , M_2O_3 and V_2O_5 mono metallic oxides, which were analyzed in the work conditions [17, 18]. TPR data are summarized in Table 2. The different reducibility of M_2O_3 ($\text{M} = \text{Fe, Cr, V}$) phases is in agreement with the reduction potentials ($E^\circ \text{Fe(III)/Fe(II)} = 0.77\text{ v}$, $E^\circ \text{Cr(III)/Cr(II)} = -0.41\text{ v}$ and $E^\circ \text{V(III)/V(II)} = -0.25\text{ v}$). This explains why only Fe(III) was easily reduced to the divalent state. Likewise, the reduction to metal iron ($E^\circ \text{Fe(III)/Fe} = -0.03\text{ v}$, $E^\circ \text{Fe(II)/Fe} = -0.41\text{ v}$) is comparatively more probable than that corresponding to Cr° and V° respectively ($E^\circ \text{Cr(III)/Cr} = -0.74\text{ v}$, $E^\circ \text{Cr(II)/Cr} = -0.56\text{ v}$ and $E^\circ \text{V(II)/V} = -1.2\text{ v}$). So, reduction to Fe° is expected at low temperature ($\sim 350^\circ\text{C}$). However, the metallic dispersion was surely high enough for a possible XRD detection. Contrary, V_2O_3 , Cr_2O_3 oxides were stable phases in the entire range of thermal treatment in our experimental conditions. The stability of end vanadium product was in agreement with the redox properties of the V(V)-V(IV)-V(III) system ($E^\circ \text{V(V)/V(IV)} \sim 1\text{ v}$ and $E^\circ \text{V(IV)/V(III)} \sim 0.33\text{ v}$, [19, 20]).

TPR profiles of the Mo(VI) oxide phases presented a common feature, pointing out that the reduction process took place, at least, by means of two stages. However, the process can be more complex, depending on the chemical composition of the phase. It is reported that Mo(VI) reduction in $\text{Fe}_2(\text{MoO}_4)_3$ started with the formation of Mo(V) and Mo(IV) at the surface of the particle. These species could be re-oxidized to Mo(VI) by the Fe(III) ions to yield Fe(II) [21]. This secondary

process ensured the stabilization of Mo(VI) as FeMoO₄. So, the presence of this oxide seemed to delay the thermal reduction of segregated MoO₃, showing a different behaviour to that observed for MoO₃ free of promoters [21]. The second TPR signal for the Fe(III)-molybdate, observed at 735 °C, could be attributed to the MoO₃-MoO₂ process. A small proportion of some other oxides (Fe₂O₃ and Fe₂Mo₃O₈) could be explained by an iron-molybdenum redox process. Finally, the last TPR signal was attributed to the formation of metal phases (Mo, Fe and Fe-Mo alloy).

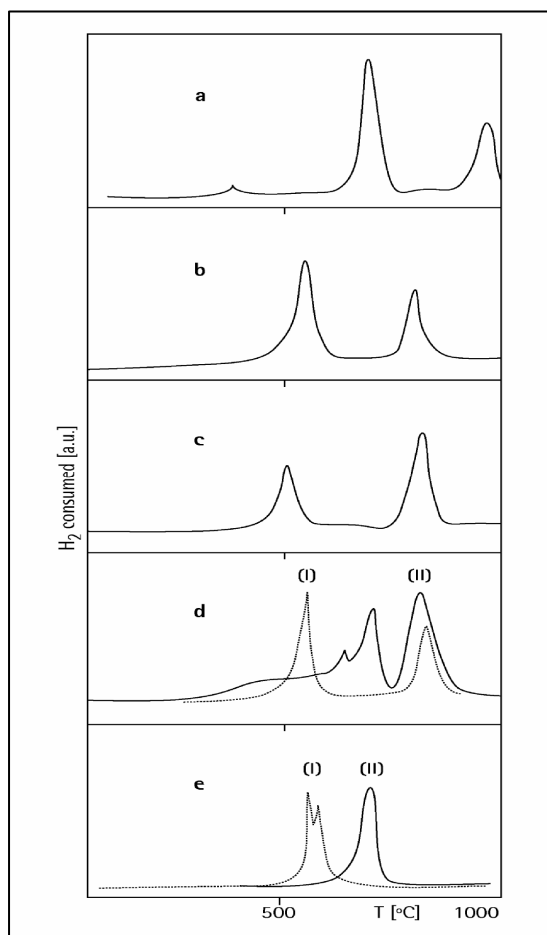


Figure 3. Comparison of TPR profile of Cr_xFe_{1-x}VMoO₇: a) x = 0; b) x = 0.5; c) x = 1; and d) (I) Cr₂(MoO₄)₃; d) (II) Fe₂(MoO₄)₃; e) (I) CrVO₄ and e) (II) FeVO₄.

Unlike Fe₂(MoO₄)₃, the Cr₂(MoO₄)₃ yielded different oxidizing phases, pointing out that the Mo(VI)-Mo(IV) reduction was more simple. Thus, MoO₂ and Cr₂O₃ were basically the majority phases from the reduction at intermediate temperature whereas Mo and Cr₂O₃ were the products at the highest temperature.

Table 2 also shows the majority reduction products of mixed oxides containing vanadium. In this sense, it is interesting to notice that CrVO₄ and FeVO₄ phases have different crystal structures and V environments (tetrahedral and octahedral respectively) [22]. Whereas FeVO₄ yielded FeV₂O₄ spinel and Fe metal at 745 °C, CrVO₄ formed a (Cr_{0.5}V_{0.5})₂O₃ solid solution at 614 °C. However, the first TPR signal, observed at 560 °C, can be assigned to the metastable Cr(III) doped-VO₂ reduced rutile-type. Cr(III)-V(III) substitution (*r* Cr= 0.615 Å, *r* V= 0.64 Å) to form (V,Cr)₂O₃ led to an increase of the rhombohedral cell volume, in agreement with that expected by Vegard's law [23].

Table 2. TPR results of mono and bi metallic oxides related to the studied systems (majority phases from XRD and FTIR spectroscopy).

T(°C) of TPR signal	MoO ₃	V ₂ O ₅	Fe ₂ O ₃	Fe ₂ (MoO ₄) ₃	Cr ₂ (MoO ₄) ₃	FeVO ₄	CrVO ₄
350			Fe ₃ O ₄ (tr)				
400-480	Mo ₄ O ₁₁ , MoO ₂ tr	VO ₂	Fe ₃ O ₄ , Fe tr	FeMoO ₄ (tr) MoO _{3-x}			
560							(V,Cr)O ₂
578					Cr ₂ O ₃ , MoO ₂		
610							(V,Cr) ₂ O ₃
630	MoO ₂						
642		V ₂ O ₃					
650			Fe				
655				FeMoO ₄			
735				MoO ₂ Fe ₂ Mo ₃ O ₈ (tr)			
745						FeV ₂ O ₄ Fe	
845	Mo						
860				Mo, Fe			
884					Cr ₂ O ₃ , Mo		

tr: traces

FTIR spectroscopy confirmed the results obtained by XRD [24]. Fig. 4 presents the FTIR spectra of Fe₂(MoO₄)₃ original (a) and reduced at 750 °C (b). In fact, the strong and broad band centered at 855 cm⁻¹ was typical of Mo(VI)-O tetrahedral stretching mode while the weak bands at 650 cm⁻¹, attributed to Fe(III)-O octahedral vibrations, practically were overlapped with the former. The weak bands observed below 450 cm⁻¹ could be assigned to Mo-O and Fe-O bending modes. A very well resolved spectrum of the FeMoO₄ (Mo octahedrally coordinated) was observed by heating at 750 °C. The improvement of the resolution was due to the reduction of free MoO₃ oxide to give MoO₂. However, the strong and sharp band at 913 cm⁻¹ was assigned to the shorter Mo(VI)-O bond of FeMoO₄. The presence of MoO₂ as majority phase and traces of Fe^{II}Mo^{IV}₃O₈ did not affect the feature of the spectrum since molybdenum dioxides, like other MO₂ rutile-type structures, are characterized by very poorly resolved spectra. In this sense, it is interesting to remark that this spectroscopic characteristic seems to be typical for a great number of oxides with very short metal-metal distances, similar to what is observed in the metallic state.

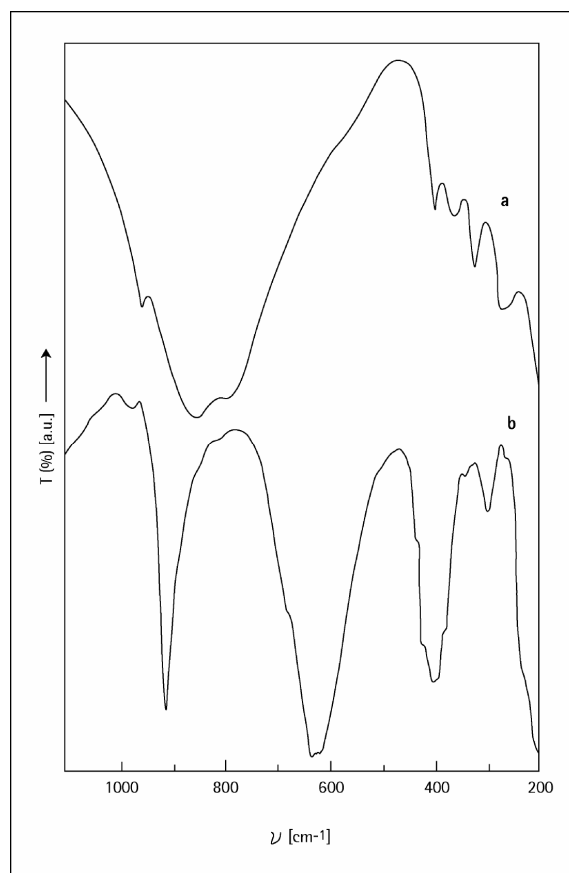


Figure 4. FTIR spectra of original and reduced Fe₂(MoO₄)₃ bimetallic phase (range 1000 to 200 cm⁻¹).

The FTIR characterization of Cr₂(MoO₄)₃ reduction process was more simple, according to what is shown in Fig. 5 (a and b). The clear difference between the FTIR spectra, (a) before and (b) after the TPR signal, corroborated the transition from Mo(VI)-O tetrahedral to Mo(IV)-O octahedral. Nonetheless, the last spectra yielded a very weak and broad band, neglected for comparative purposes but useful to demonstrate the course of reduction. Thus, spectrum of Fig. 5 (b) practically corresponded to that of Cr(III) oxide [25].

At this point, it is interesting to observe that the different thermal reduction behaviors of Cr and Fe end members of the (Fe,Cr)VMoO₇ solid solution, shown in Fig. 3 (a and c), can be attributed to the M(III) redox properties. The products (from XRD and FTIR results) and the temperature of TPR signals are summarized in table 3. It is evident that metal connectivity, polarization and electronegativity in the original phase as well as the stability of reduction products play a definite role. It is also evident that the simultaneous presence of two types of M(III) ions affected even more the stability of the lattice, situation that was completely defined by the expected ordered structure for Cr_{0.5}Fe_{0.5}VMoO₇. In fact, while other intermediate solid solutions did not yield very precise TPR signals, the temperature of the first signal diminished up to 515 °C when the Fe/Cr=1. The behaviour could be referred as a mutual and appropriate promotion effect in the lattice since the energy needed to remove oxygen from the network is lower when the M₂O₁₀ dimer is constituted by two different species. Some reported studies on instabilities of oxide lattices containing Mo and V reveal that the metal-metal interaction is associated to a near equivalence of the electron-nuclear and electron-electron interatomic interactions at two neighbouring metallic sites [26].

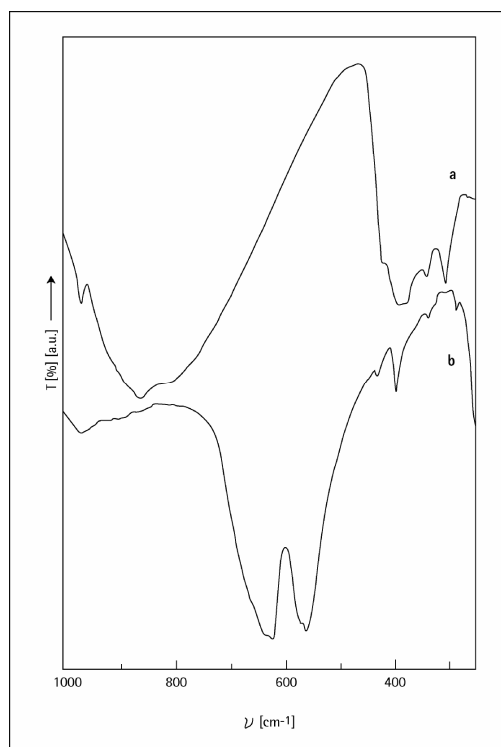


Figure 5. FTIR spectrum of original and reduced $\text{Cr}_2(\text{MoO}_4)_3$ at 560 $^\circ\text{C}$ (range 1000 to 200 cm^{-1}).

Table 3. TPR data of FeVMoO_7 , $\text{Cr}_{0.5}\text{Fe}_{0.5}\text{VMoO}_7$ and CrVMoO_7 members of the solid solution (majority products from XRD and FTIR spectroscopy).

T ($^\circ\text{C}$)	FeVMoO_7	$\text{Cr}_{0.5}\text{Fe}_{0.5}\text{VMoO}_7$	CrVMoO_7
360	$\text{Fe}_3\text{O}_4?$		
515		FeMoO_4 , MoO_2 , $(\text{V,Cr})_2\text{O}_3$	
560			$(\text{V,Cr})_2\text{O}_3$, MoO_2
704	FeV_2O_4 , MoO_2 , Fe (tr) $\text{FeMoO}_4?$		
838			$(\text{V,Cr})_2\text{O}_3$, Mo
852		FeV_2O_4 , $(\text{V,Cr})_2\text{O}_3$, Fe, Mo	
1005	FeV_2O_4 , Mo, Fe		

(tr) traces

For the end members, a particular affinity between M and V atoms can be associated to the structural feature. The re-arrangement occurs among the involved polyhedra along the layer-like nets, constituted by M_2O_{10} and VO_4 units (plane A in the “ideal” structural projection of Fig.1

whereas the MoO₄ units, are in a position relatively less linked. According to the structural feature, for the end members of the isomorphous, prevail the formation of the Fe^{IV}V₂^{III}O₄ and (V^{III},Cr^{III})₂O₃ prevailed, segregating the MoO₂ rutile-type oxide. Contrary, for the intermediate member containing (CrFe)O₁₀ units a different behaviour was observed. It is attributed to the different polarizing effects of M(III) species which are responsible of the dimmer distortion.

Additional experiences were made from physical mixtures of V₂O₅ and Fe₂O₃ oxides to give FeVO₄ and of V₂O₅ and Fe₂(MoO₄)₃ to give FeVMoO₇. Results showed the formation of FeV₂O₄ at ~650 °C whereas VO₂ and FeMoO₄ were obtained at 480 °C.

Finally, the formation of the (Cr_{1-x}V_x)₂O₃ solid solution at 560 °C was supported by XRD analysis from the calculated cell volume (from XRD measurements) which led to an x value of ~0.4 according to Vegard's law. The previous formation of a MoO₂-VO₂ solid solution (rV(IV)= 0.58 Å, r Mo(IV)= 0.65 Å) cannot be confirmed [9] unlike the one observed in the CrVO₄ reduction. Unfortunately, the quality of the sample was not so good as to obtain an XRD accurate measurement. Likewise, the crystallinity of the samples was not improved due to the small stability range of V(IV) in the experimental conditions.

SEM micrograph of Fig. 6 a) corresponds to the typical morphology of the studied phases while Fig. 6 b) corresponds to the Fe rich end member treated at 800 °C. The other reduced phases reveal alterations, according to the chemical composition. Table 4 presents the EDS data for all the studied phases. The Fe-rich phase shows a Mo increase and a Fe decrease whereas in the other members the metal contents remain practically unchanged. These results suggested that the reduction process up to ~ 600°C can be interpreted by the shrinking core model with a different rate of crystal growth for each segregated oxide, according to the composition.

Table 4. Metallic contents (as % wt) by EDS at different reduction stages of the Fe_{1-x}Cr_xVMoO₇ solid solution.

Stage	Fe (% wt)	Cr (% wt)	V (% wt)	Mo (% wt)
(1)FeVMoO ₇ ^a	27.5		25.1	47.3
750°C ^b	20.7		27.8	51.5
1000°C ^c	15.4		28.8	55.7
(2)Fe _{0.5} Cr _{0.5} VMoO ₇ ^a	14.0	13.0	25.3	47.8
560°C ^b	9.9	14.7	24.8	50.5
900 °C ^c	8.7	14.4	25.7	51.1
(3)CrVMoO ₇ ^a		26.1	25.6	48.2
600°C ^b		27.0	25.4	47.5
900°C ^c		28.3	24.4	47.3

Theoretical values: (1) Fe 27.55, V 25.13, Mo 47.32 ; (2) Fe 13.90, Cr 12.95, V 25.37, Mo 47.78;

(3) Cr 26.14, V 25.62, Mo 48.24

^a Original phase; ^b Temperature of end of TPR first stage; ^c Temperature of end of TPR second stage.

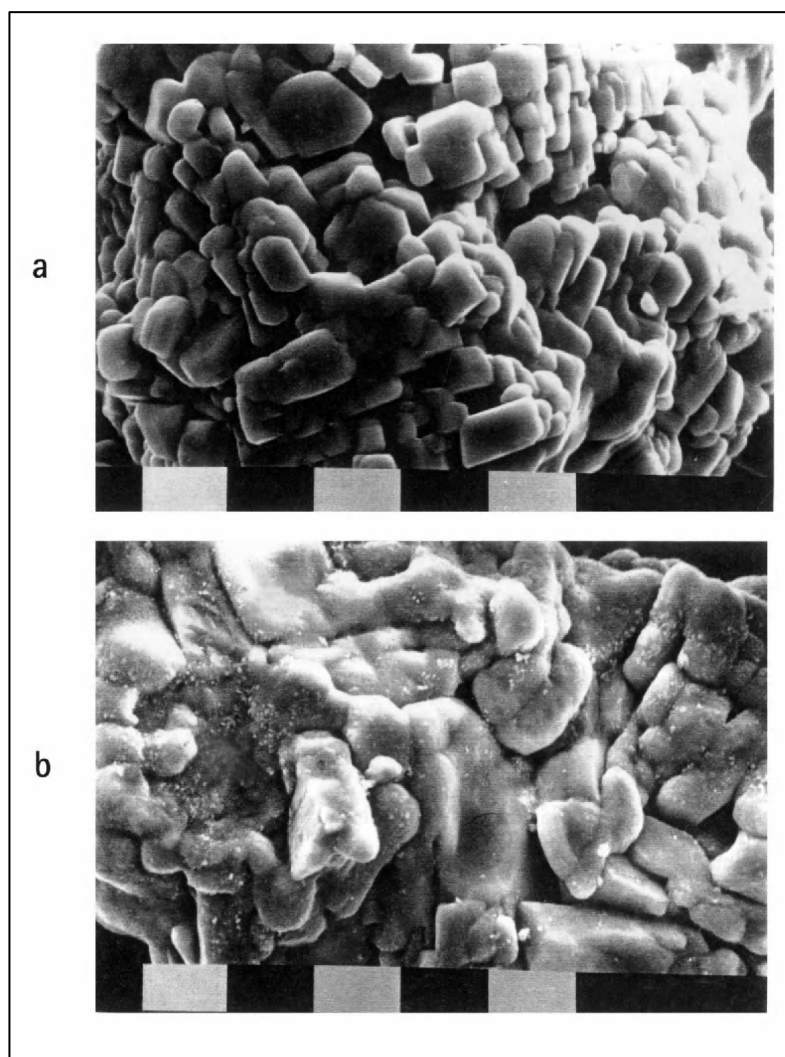


Figure 6. SEM micrograph of triclinic phases: a) FeVMoO_7 and b) product of the thermal treatment at 800°C , (magnification $\times 1620$, scale bar = $10\mu\text{m}$).

III- Catalytic potential of the $(\text{Fe,Cr})\text{VMoO}_7$ phases

On the basis of the interest of physical mixtures of V, Fe and Mo oxides as catalysts of oxidation processes, the studied members of the $(\text{Fe,Cr})\text{VMoO}_7$ solution were tested in a typical oxidation reaction, despite the low specific surface area ($\sim 15\text{ m}^2/\text{g}$). It is well known that the methanol is widely used as a probe molecule to study catalytic surfaces. From the formed products the properties of the adsorption – oxidation sites can be inferred: dimethyl ether was formed by surface acid sites; CO_2 was formed by surface basic sites whereas formaldehyde, methyl formate and dimethoxy methane and CO resulted from the surface redox sites. So, the Study of the Transients of the Methanol Oxidation was performed by Mass Spectrometry. In this sense, the masses of 28, 30, 31, 44 and 45 were taken as representatives of CO, formaldehyde, methanol, CO_2 and dimethyl-ether molecules respectively.

It was observed that the oxide phases revealed neither interaction nor adsorptive process with methanol below 400°C . However at this temperature, they quickly interacted resulting in formaldehyde as majority product and CO, CO_2 and dimethyl-ether as minority products despite being strongly influenced by the chemical composition of oxidic phases (transients).

This behaviour confirmed the high stability of these condensed structures in the RT- 400 °C range, where the electronic transfer was not possible.

Table 5 shows the mass intensities corresponding to the reactive in excess (without reaction) and to the different oxidation products (expressed in %) by using the three catalytic phases.

Figure 7 shows desorption spectra of methanol pulses over FeVMoO₇ for mass intensity of formaldehyde at 400 °C. The Fe-rich phase yielded greater amounts of formaldehyde, CO and CO₂ and a smaller amount of methanol without reacting compared to the other samples.

Table 5. Mass intensities corresponding to the reactive in excess (without reaction) and to the different oxidation products (expressed in %) by using the three catalytic phases.

Catalyst	Methanol (%)	Formaldehyde (%)	Dimethyl Ether (%)	CO (%)	CO ₂ (%)
FeVMoO ₇	13	56	--	28	3
Fe _{0.5} Cr _{0.5} VMoO ₇	66	20	1	13	0.1
CrVMoO ₇	67	22	0,8	10	0.1

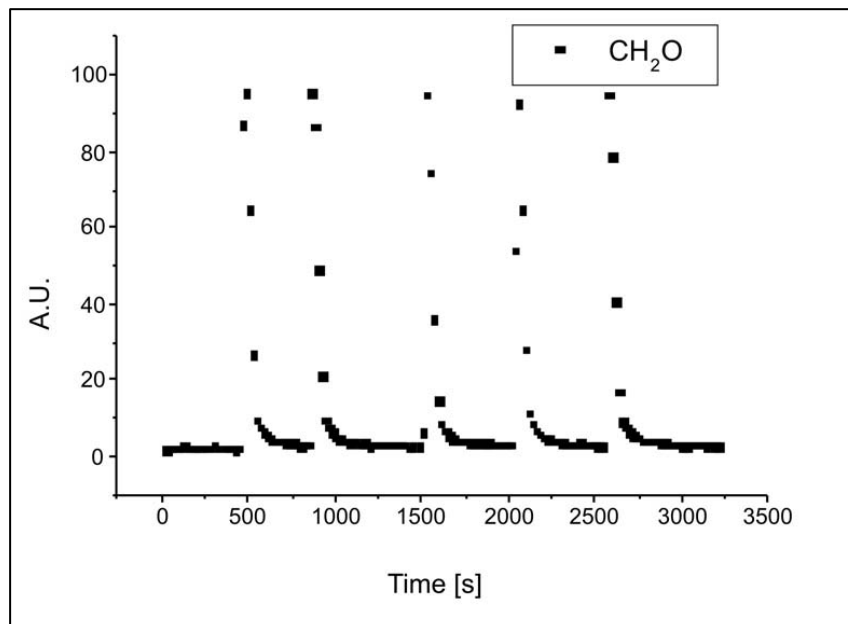


Figure 7. Desorption spectra of methanol pulses over FeVMoO₇ for mass intensity of formaldehyde. Experimental temperature: 400°C.

The presence of Cr in the lattice affects the catalytic behaviour in a similar way with a very low production of formaldehyde. Additionally, unreacted methanol and a little amount of dimethyl-ether were observed.

Considering the fast adsorption process, methanol coordinated to a transition metal by H-elimination yielded the formation of methoxy species, which were quickly desorbed as formaldehyde or other products due to the high temperature. It is interesting to indicate that in V_2O_5 the formaldehyde desorption occurred at 192 °C [27].

Structural features of studied phases (presence of trivalent dimmers) allow the fast electron exchange between the central metals, facilitating the coexistence of Fe(II) and Fe(III) oxidation states, both stables in octahedral coordination. This effect can be related to that observed in other stable oxide system i.e. magnetite which has electronic conductivity equivalent to metals [28, 29].

Fig. 8 shows desorption spectra of methanol pulses over $FeVMoO_7$ for oxygen and methanol at 400 °C. This experience was carried out with oxygen impurity of He, according to the fast Mars-van Krevelen mechanism [30].

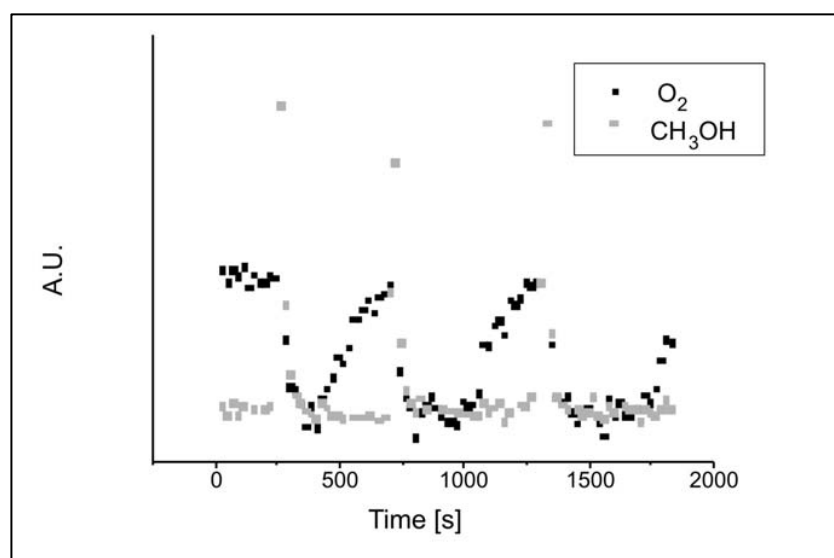


Figure 8. Desorption spectra of methanol pulses over $FeVMoO_7$. Mass intensities are shown for oxygen and methanol. Experimental temperature: 400°C.

Regarding the oxidizing power of phases containing Cr, their behaviour was similar but clearly lower than that observed for the Fe rich end member. The poor oxidising power, in the intermediate composition ($Cr_{0.5}Fe_{0.5}$) can be related to the lower electronic conductivity confirming the ordered distribution of the trivalent metal in the dimmers $(Fe,Cr)O_6$. The replacement Cr-Fe prevented the quick electron exchange, showing a behaviour similar to that of Cr-rich end phase. This fact was also observed by the $CrVMoO_7$ and $(Cr_{0.5}Fe_{0.5})VMoO_7$ TPR patterns.

The presence of acid sites in the samples with Cr was revealed by small amounts of dimethyl ether production, which was in agreement with the main property of this oxide in the methanol reaction [11]. The replacement Cr-Fe in the isomorphous structure decreased the catalytic potential for the methanol oxidation. Likewise, it led to a lower selectivity to formaldehyde, pointing out that Fe was the principal actor in their oxidizing power. It is also interesting to observe that the tetrahedral V in the condensed multimetallic phase did not present the reactivity of binary V_2O_5 , in spite of the presence of a short bond V-O of similar value.

Conclusions

As a main conclusion, catalytic, structural and reducing behaviour can be correlated supporting the performance of the phases in the catalytic methanol oxidation process. It can be underlined the role that the Fe(III) reducibility and the presence of the structural M₂O₁₀ dimer played in this multimetallic and condensed catalytic system. The co-existence of iron in both oxidation states in close octahedral sites facilitated the electronic transfer and increased the activity and selectivity toward the formaldehyde formation. However, unlike the effect observed for the end members of the series, the Cr-Fe ordered distribution in the dimer for the Cr_{0.5}Fe_{0.5}VMoO₇ intermediate member, clearly revealed a M(III) displacement from the centre of MO₆ linked polyhedra, with a distortion that affected the structural stability and led to the formation of the FeMoO₄ as intermediate phase, in a similar behaviour to that observed in other Fe(III)-Mo(VI)-O catalytic systems.

Acknowledgments. We are grateful to Mrs. Graciela Valle, for their contribution in experimental measurements. Authors would like to thanks the financial support from CONICET, UNLP, ANPCyT and CICPBA (Argentina).

References

- [1] B. Ramachandra, J. Sik Choi, K-Y. Choo, J-S. Sung, S. Dal Song, T.H. Kim, *Cat. Lett.* **2005**, *105*, 23.
- [2] F. Trifiro, F. Forzatti P., P.L. Villa, in: B. Delmon, P. Jacobs, G. Poncelet (Eds.), *Preparation of Catalysts*, Elsevier, Amsterdam, 1976, pp. 147.
- [3] M. del Arco, C. Martin, V. Rives, A.M. Esteves, M.C. Marques, A.F. Tena, *Mater. Chem. Phys.* **1989**, *23*, 517.
- [4] R.A. Sheldon, J.K. Kochi, “*Metal Catalyzed Oxidations of Organic Compounds*”, Academic Press, New York, 1981, pp. 153.
- [5] J.M.M. Millet, H. Ponceblanc, G. Coudurier, J.M. Herrmann, J.C. Vedrine, *J. Catal.* **1993**, *142*, 381.
- [6] I. Laligant, L. Permer, A. Le Bail, *Eur. J. Solid State Inorg. Chem.* **1995**, *32*, 325.
- [7] J. Walczak, P. Tabero, E. Filipek, *Thermochim. Acta* **1996**, *275*, 249.
- [8] K. Knorr, P. Jakubus, J Walczak, E. Filipek, *Europ. J. Solid State Inorg. Chem.* **1998**, *35*, 161.
- [9] R.D. Shannon, *Acta Crystallogr. Sect. A* **1976**, *32*, 751.
- [10] M.C. Prieto, J.M. Gallardo Amores, V. Sanchez Escribano, G. Busca, *J. Mater. Chem.* **1994**, *4*, 1123.
- [11] M. Badlani, I.E. Wachs, *Catal. Let.* **2001**, *3-4*, 75.
- [12] M.B. Vassallo, I.L. Botto, *Thermochim. Acta* **1996**, *279*, 205.
- [13] T. J. B. Holland, S.A.T. Redfern, *Mineralogical Magazine* **1997**, *61*, 65.
- [14] V. Sanchez Escribano, J.M. Gallardo Amores, E. Finocchio, M. Daturi, G. Busca, *J. Mater. Chem.* **1995**, *5*, 1943.
- [15] S. Music, S. Popovic, M. Ristic, *J. Mater. Sci.* **1993**, *28*, 632.
- [16] N. Khosrovani, A.W. Sleight, *J. Solid State Chem.* **1996**, *121*, 2.
- [17] A. Jones, B. Mc Nicol, *Temperature Programmed Reduction for Solid Materials Characterization*, Marcel Dekker Inc., New York, 1984.
- [18] I.L. Botto, C. I. Cabello, H. J. Thomas, *Mat. Chem. and Physics* **1997**, *47*, 37.

- [19] L.E. Briand, L. Gambaro, H.J. Thomas, *J. Thermal Anal.* **1995**, *44*, 803.
- [20] N.H. Hurst, S.J. Gentry, A. Jones, B.D. Mc Nicol, *Catal. Rev. Sci. Eng.* **1982**, *24*, 233.
- [21] H. Zhang, J. Shen, X. Ge, *J. Solid State Chem.* **1995**, *117*, 127.
- [22] M. Touboul, K. Melghit, *J. Mater. Chem.*, **1995**, *5*, 147.
- [23] I.L. Botto, M. Vasallo, M. Occhiuzzi, D. Cordischi, P. Porta, *J. Solid State Chem.* **1999**, *144*, 392.
- [24] E.J. Baran, I.L. Botto, *Monatsh. Chem.* **1997**, *108*, 311.
- [25] J.B. Goodenough, A. Manthiram, G. Dutta, *Europ. J. Solid State and Inorg. Chem.* **1991**, *28*, 1125.
- [26] J. Preudhomme, P. Tarte, *Spectrochim. Acta.* **1971**, *27 A*, 1817.
- [27] L. Gambaro, *J. Mol. Catal. A Chem.* **2004**, *287*, 214.
- [28] R. Bauminger, S.G. Cohen, A. Marinov, S. Ofer, E. Segal, *Phys. Rev.* **1961**, *122(5)*, 1447.
- [29] A. Ito, K. Ono, Y. Ishikawa, *J. Phys. Soc. Japan*, **1962**, *17 (Suppl. B1)*, 125.
- [30] J.C. Vedrine, G. Coudurier and J.M. Millet, *Catal. Today* **1997**, *33*, 3.